2007

Biostimulation of iron reduction and subsequent oxidation of sediment containing Fe-silicates and Fe-oxides: Effect of redox cycling on Fe(III) bioreduction

John Komlos
Princeton University, jkomlos@princeton.edu

Ravi K. Kukkadapu
Pacific Northwest National Laboratory, ravi.kukkadapu@pnl.gov

John M. Zachara
Pacific Northwest National Laboratory, john.zachara@pnl.gov

Peter R. Jaffe
Princeton University, jaffe@princeton.edu

WATER RESEARCH 41 (2007) 2996–3004

Available at www.sciencedirect.com

ScienceDirect

journal homepage: www.elsevier.com/locate/watres

Biostimulation of iron reduction and subsequent oxidation of sediment containing Fe-silicates and Fe-oxides: Effect of redox cycling on Fe(III) bioreduction

John Komlos[a], *Ravi K. Kukkadapu*[b], *John M. Zachara*[b], *Peter R. Jaffé*[a,*]

[a]*Department of Civil and Environmental Engineering, Princeton University, Princeton, NJ 08544, USA*
[b]*Pacific Northwest National Laboratory, Richland, Washington, DC 99352, USA*

ARTICLE INFO

Article history:
Received 18 October 2006
Received in revised form
12 March 2007
Accepted 13 March 2007
Available online 27 April 2007

Keywords:
Iron
Reduction
Oxidation
Fe-silicates
Cycling
Manganese

ABSTRACT

Sediment containing a mixture of iron (Fe)-phases, including Fe-oxides (mostly Al-goethite) and Fe-silicates (illites and vermiculite) was bioreduced in a long-term flow through column experiment followed by re-oxidation with dissolved oxygen. The objective of this study was (a) to determine the nature of the re-oxidized Fe(III), and (b) to determine how redox cycling of Fe would affect subsequent Fe(III)-bioavailability. In addition, the effect of Mn on Fe(III) reduction was explored.[57]Fe-Mössbauer spectroscopy measurements showed that biostimulation resulted in partial reduction (20%) of silicate Fe(III) to silicate Fe(II) while the reduction of goethite was negligible. Furthermore, the reduction of Fe in the sediment was uniform throughout the column. When, after biostimulation, 3900 pore volumes of a solution containing dissolved oxygen was pumped through the column over a period of 81 days, approximately 46% of the reduced silicate Fe(II) was re-oxidized to silicate Fe(III). The Mössbauer spectra of the re-oxidized sample were similar to that of pristine sediment implying that Fe-mineralogy of the re-oxidized sediment was mineralogically similar to that of the pristine sediment. In accordance to this, batch experiments showed that Fe(III) reduction occurred at a similar rate although time until Fe(II) buildup started was longer in the pristine sediment than re-oxidized sediment under identical seeding conditions. This was attributed to oxidized Mn that acted as a temporary redox buffer in the pristine sediment. The oxidized Mn was transformed to Mn(II) during bioreduction but, unlike silicate Fe(II), was not re-oxidized when exposed to oxygen.

1. Introduction

Microbial reduction of iron (Fe) has been shown to be important in the transformation and remediation of contaminates in groundwater such as radionuclides (e.g., Anderson et al., 2003; Fredrickson et al., 2004; Istok et al., 2004) and petroleum hydrocarbons (e.g., Anderson et al., 1998; Tuccillo et al., 1999; Zachara et al., 2004). Re-oxidation of microbially reduced Fe may occur in sediments that experience oxidation–reduction cycling (e.g., seasonal groundwater fluctuations) and can thus impact the duration of contaminant remediation. Multiple Fe phases can be present in sediments, including amorphous/poorly crystalline Fe(III)-oxides (e.g., ferrihydrite), highly crystalline Fe(III) oxides and

*Corresponding author. Tel.:+1 609 258 4653; fax: +1 609 258 2799.
E-mail addresses: jkomlos@princeton.edu (J. Komlos), Ravi.Kukkadapu@pnl.gov (R.K. Kukkadapu), john.zachara@pnl.gov (J.M. Zachara), jaffe@princeton.edu (P.R. Jaffé).
0043-1354/$ - see front matter © 2007 Elsevier Ltd. All rights reserved.
doi:10.1016/j.watres.2007.03.019

Fe(II)/(III)-silicates/clays. All of these Fe phases have been shown to be bioreducible to various degrees under different scenarios (e.g., Tuccillo et al., 1999; Larsen and Koch, 2000; Kukkadapu et al., 2001, 2006; Fredrickson et al., 2004; Zachara et al., 2004; Cooper et al., 2005; Roden and Zachara, 1996; Peretyazhko and Sposito, 2005; Favre et al., 2006). Various forms of biogenic Fe(II) may exist—aqueous Fe(II), Fe(II) adsorption complexes on mineral surfaces (Larsen and Koch, 2000), mineral precipitates or sorbed Fe (Kukkadapu et al., 2001; Peretyazhko and Sposito, 2005), and structural Fe(II) (Gates et al., 1996; Jaisi et al., 2005) that may re-oxidize and transform at different rates and extent in the presence of oxygen. Little research, however, has been performed to examine the extent and mineral changes involved during the reduction and subsequent re-oxidation of biogenic Fe, and how these changes will affect Fe bioavailability during oxidation/reduction cycling. Introduction of oxygen (i) may only re-oxidize adsorbed or sorbed Fe(II) on the outer surface of the sediments, thus forming an Fe(III) oxide shell that protects Fe(II) (and other reduced species) underneath the Fe(III) from further oxidation, (ii) may simply re-oxidize the reduced Fe(II) in clays, and/or (iii) may not be effective in oxidizing Fe(II) immobilized in the oxide structure [e.g., Fe(II) in magnetite]. In scenarios (i) and (ii), re-oxidation of bioreduced Fe(II) may yield an Fe(III) phase very different than the initial one, thus potentially affecting the subsequent rate and extent of Fe reduction.

In addition, manganese (Mn) (if any present and mixed with the sediment) can also influence Fe-cycling. For example, reducible Mn(III)/(IV)-oxides have been shown to act as a temporary redox buffer and delay the onset of Fe reduction (Fredrickson et al., 2004) though it is unclear how Mn mineralogy will change during redox cycling and if Mn will influence Fe(III) reduction in the re-oxidized sediment. Research performed regarding the effect of Mn on Fe cycling (e.g., Canfield et al., 1993; Van Cappellen and Wang, 1996) has mostly been done in marine environments and has not focused on Mn/Fe cycling in saturated groundwater systems where biological processes are employed for contaminant remediation. The Mn(II) produced during Mn reduction may be soluble and be transported from the system. Alternatively, the Mn(II) may remain surface bound and re-oxidize when oxygen is introduced to the system, thus continuing to affect the onset of Fe-reducing conditions in the re-oxidized sediment.

Therefore, reduction and subsequent re-oxidation of sediment could have a profound effect on Fe-reducing conditions. A greater understanding of these interactions can have a significant impact on bioremediation scenarios in these environments where Fe reduction has been linked to contaminant degradation. The objective of the research described here was to determine how the Fe mineralogy of sediment containing Fe(III)-oxides, Fe(II)/Fe(III)-silicates, and Mn-oxides changes as it is cycled through biological reduction and subsequent re-oxidation in field relevant conditions (flow-through sediment columns). Key to this research is the determination of which Fe fractions are actually reduced/oxidized and how the Fe mineralogy of the re-oxidized sediment compares to the initial sediment and hence how the bioavailability of the Fe(III) is affected by reduction/oxidation cycling. In addition, this research explored how Mn cycling influences microbial Fe(III) reduction.

2. Material and methods

2.1. Sediment description

The sediment used was obtained from the uncontaminated background area of the Office of Biological and Environmental Research (OBER) Field Research Center (FRC) located within the Y-12 Plant area on the Department of Energy's (DOE's) Oak Ridge Reservation in Oak Ridge, Tennessee. The sediment was collected at depths between 36″ and 72″ below ground surface and stored at 4 °C until its use. No additional preparation (drying, sieving) was performed.

2.2. Sediment reduction via biostimulation

The sediment used in the re-oxidization column experiment was biologically reduced in a column experiment previously described in Komlos and Jaffé (2004). Briefly, a 30 cm long × 5 cm diameter polycarbonate column was filled with FRC sediment and supplied a phosphate buffered (PB; 10 mM) solution (0.4 g KH_2PO_4, 1.23 g K_2HPO_4, 10 mL vitamin solution (Lovley and Phillips, 1988a) and 10 mL trace minerals solution (Lovley and Phillips, 1988a) per liter of distilled water) up-flow through the column at a rate of 0.5 (±0.025) mL/min. The column was equipped with sampling ports every 2 cm along the length of the column. Each sampling port had an SGE luer lock stainless steel needle (50 mm, 23 ga., pt#2, Supelco) that extended into the middle of the column. A syringe pump (KD Scientific) supplied an acetate concentration of 3 mM to the column. The column was operated at 30 °C until it was destructively sampled in an anaerobic glove box (3:97 H_2:N_2) and Fe concentrations quantified along the length of the column.

2.3. Fe re-oxidation column experiment

A 2.5 cm diameter, 15 cm long glass column (Kimble Kontes) was filled inside an anaerobic glove box with 120 g of the bioreduced sediment from between 10 cm and 20 cm of the column and transferred to a walk-in temperature controlled chamber (30 °C) where PB solution (constantly stirred to maintain equilibrium with ambient atmosphere) was pumped up-flow through the column at a rate of 0.35 mL/min. A Corning 317 dissolved oxygen (DO) meter was fitted to an in-line sampling device attached to either the influent or effluent of the column that allowed for DO to be measured over time. A conservative tracer (bromide) breakthrough curve was performed during the column experiment by adding 40 mg/L bromide to the influent media and measuring its concentration at the effluent. Bromide was detected using a Dionex DX500 ion chromatograph with a CD25 conductivity detector and a Dionex IonPac AS14-4 mm column. At the termination of the experiment, the column was destructively sampled in an anaerobic glove box by removing the end cap and incrementally removing sediment samples every 1–2 cm

with a long spatula and quantifying for Fe content as described below.

2.4. Batch bioreduction experiments

Batch experiments were performed to compare the rate of Fe reduction in the re-oxidized sediment to that measured in the pristine (original) sediment. Two different experiments were performed; one with anthraquinone 2,6 disulfonate (AQDS; Sigma-Aldrich) and one without AQDS. For each experiment, the pristine sediment was bioreduced in batch mode at the same time (and with the same culture) as the re-oxidized sediment. A description of the experimental set-up is as follows. One gram of either pristine or re-oxidized sediment was added to crimp-seal test tubes with 9 mL of PB solution and sealed with a butyl rubber stopper (Fisher Scientific). The tubes were purged with CO_2/N_2 gas (20:80) for 15 min. One mL of a *Geobacter sulfurreducens* growth culture was added to each tube to ensure that both sediments contained a significant quantity (7×10^6 cells/mL) of an active Fe-reducing population. The growth culture was prepared by growing *G. sulfurreducens* on acetate and ferric citrate for 5 days in a bicarbonate buffered growth media prepared as previously described (Komlos and Jaffé, 2004). After 5 days, the growth culture was rinsed to remove aqueous Fe(II) by centrifuging (5900*g*) for 20 min, anaerobically removing the supernatant and replacing with PB solution purged with CO_2/N_2 gas (20:80). *G. sulfurreducens* was chosen because microorganisms with 16S rDNA sequences closely related to *G. sulfurreducens* have been isolated from the FRC during biostimulation (Peacock et al., 2004) and are important organisms in subsurface environments experiencing bacterial Fe(III) reduction (Anderson et al., 2003). Sodium acetate was added to yield concentrations of 10 mM acetate. AQDS, an electron shuttle that has been shown to enhance the rate and extent of Fe reduction in this sediment (Komlos and Jaffé, 2004, Kukkadapu et al., 2006), was added in certain incubations to a final concentration of 0.05 mM. The tubes were placed on a slow moving (7 rpm) rotator in a 30 °C incubator and Fe(II) concentrations were monitored over time as described below.

2.5. HCL-extractable Fe

HCl-extractable Fe concentrations were measured as described below using different variations of the 0.5 N HCl extraction/ferrozine detection method (Lovley and Phillips, 1987; Komlos and Jaffé, 2004; Anderson et al., 1998). The Fe(II) concentration in the batch experiments was measured by removing 0.1 mL of sample suspension and adding to 5 mL of 0.5 N HCl. After 1 h at room temperature, 0.1 mL of sample/HCl suspension was transferred to 5 mL ferrozine solution, mixed for 15 s, filtered using a 0.2 μm nylon filter, and analyzed using a Spectronic Genesys 2 spectrophotometer ($\lambda = 562$ nm).

In-situ measurement of biogenic Fe(II) concentrations was performed as described previously (Komlos and Jaffé, 2004). Briefly, the sediment was locally disturbed at a sampling port by extracting 0.5 mL pore water via syringe and re-injecting it back into the column. A half mL of the now suspended sediment/pore water solution was then extracted and added to 2.0 ml of 0.5 N HCl. After 1 h, 0.1 mL of sample/HCl was transferred to 5 mL ferrozine and analyzed as described above. To quantify the dry weight of this slurry, the sediment resuspending procedure was performed with a separate 0.5 mL suspended sediment/pore water sample added to a pre-weighed aluminum dish that was dried at 103 °C for 1 h and re-weighed. For each sampling point at each time point, the Fe(II) and dry weight analysis was performed in duplicate when the Fe(II) concentrations were low (before 100 d) and in triplicate later in the experiment when Fe(II) concentrations increased (after 100 d). The standard deviation of the dry weight and Fe(II) content was, on average, 20% and 34% of the mean, respectively.

HCl-extractable Fe(II) concentrations [HCl-Fe(II)] were measured at the termination of the column experiments in the anaerobic glove box by adding a known weight of sediment slurry (~0.1 g) to 5 mL 0.5 N HCl, extracting for 21–22 h and detecting as described above. Moisture contents were obtained by weighing a sediment sample before and after drying at 103 °C for 1 h. Total 0.5 N HCl extractable Fe [HCl-Fe] was quantified similarly to the above method for HCl-Fe(II) analysis except hydroxylamine hydrochloride was added to the 0.5 N HCl at a final concentration of 0.25 N prior to sediment addition. All samples were stored in the dark during extraction. 0.5 N HCl extractable Fe(III) [HCl-Fe(III)] was determined as the difference between HCl-Fe and HCl-Fe(II).

2.6. Mn analysis

Mn(II) and total Mn were extracted from sediment samples in 0.5 N HCl for 24 h. The total Mn samples also contained 0.25 N hydroxylamine hydrochloride to reduce any Mn-oxides to Mn(II). Mn(II) was detected using a Dionex DX500 ion chromatograph with a Dionex IonPac CS5A-4 mm column and absorbance detection (530 nm) after postcolumn mixing with 0.12 g 4-(2-pyridyiazo)resorcinol monosodium salt hydrate (Sigma-Aldrich) per liter of MetPac PAR Postcolumn Reagent (Dionex). The eluent (20% MetPac PDCA Eluent Concentrate [Dionex], 80% de-ionized water) and postcolumn flow rates were 1.2 and 0.7 mL/min, respectively. The oxidized Mn concentration was obtained from the difference between the total Mn and the Mn(II) concentrations. Statistical analysis was performed where indicated using two-sample *t*-tests (unequal variance). Data sets were considered significantly different if the *p*-values were lower than 0.05.

2.7. Mössbauer spectroscopy

The structural and mineralogical environment of Fe(II) and Fe(III) in pristine, bioreduced, and bioreduced/re-oxidized sediments was monitored by ^{57}Fe transmission Mössbauer spectroscopy at 12 K. Randomly oriented absorbers were prepared by mixing ~0.1 g of dried sample with petroleum jelly. The prepared Mössbauer disks were stored at −80 °C in an anoxic chamber until analysis. The sample preparation procedure and instrumentation were reported by Kukkadapu et al. (2006). A closed-cycle cryostat (ARS, Allentown) was employed for 12 K measurements. The Mössbauer data were modeled with the *Recoil* software (University of Ottawa, Canada) using a Voigt-based spectral fitting routine (Rancourt

and Ping, 1991). The coefficients of variation of the spectral areas of the individual sites generally ranged between 1% and 2% of fitted values.

3. Results and discussion

3.1. *Pristine sediment characterization*

Characterization of the Fe phases in the pristine (also in the reduced and the re-oxidized) sediment was primarily performed using ^{57}Fe transmission Mössbauer spectroscopy at 12 K (Fig. 1). At this temperature, Fe(III)-oxides (e.g., "crystalline" ferrihydrite, goethite) that display sextet features are well resolved from doublets resulting from silicate/clay Fe(II) and Fe(III) (Murad and Cashion, 2004). The Mössbauer spectrum of the pristine sediment (Fig. 1a) indicated that the majority (90%) of the Fe was in the form of Fe(III), either as Fe(III)-oxide (55%, Al-substituted goethite [major sextet feature] with minor hematite [minor sextet]) or Fe(III)-silicate (35%—inner doublet, mostly illite/vermiculite). The remaining 10% of the sediment Fe was in the form of silicate-Fe(II) (outer doublet). The silicate Fe(II)/Fe(III) ratio of the sediment was ~0.3. The identification of goethite and illite/vermiculite as primary Fe repository was based on selective chemical analysis, X-ray diffraction, transmission electron microscopy, and variable temperature Mössbauer measurements performed during another study (Kukkadapu et al., 2006). HCl-Fe(III) (1 h extraction) from the pristine sediment (10.9 ± 2.9 μmol/g dry sediment (Komlos and Jaffé, 2004)) was only a small amount (1.5%) of the total Fe (820 μmol/g sediment; Fredrickson et al., 2004), which indicated little or no ferrihydrite in the sediment. Though the pristine sediment contained a significant amount of Fe(II) as Fe(II)-silicate (10%, Fig. 1a), very little of this was extractable (0.05%) in 0.5 N HCl (Table 1).

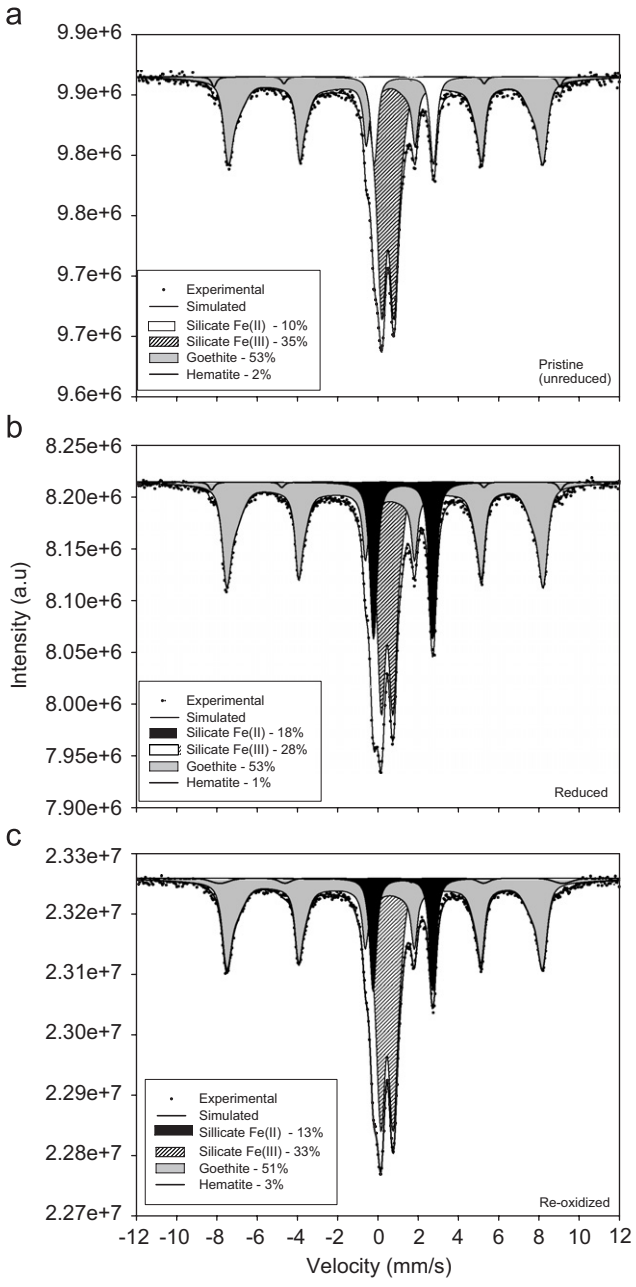

Fig. 1 – Mössbauer spectra (12 K) of the (a) pristine sediment, (b) reduced sediment and (c) re-oxidized sediment.

3.2. *Sediment reduction via biostimulation*

The sediment was reduced in a long-term column experiment where Fe reduction was first detected after 32 days of acetate addition and continued at a rate of 0.17 μmol/g sediment/d until leveling after 250 days of column operation (Fig. 2). Fe(II) was not detected in the pore water at the effluent of the column (Komlos and Jaffé, 2004). Column operation was discontinued (day 497) after biogenic Fe(II) accumulation appeared to level off and the Fe was quantified along the length of the column (Fig. 3). The biogenic HCl-Fe(II) concentration throughout the column after bioreduction (Fig. 3) was greater than the initial (pristine) HCl-Fe(III) (Table 1). The Mössbauer spectrum of the bioreduced sediment (Fig. 1b) displayed a significant (20%) decrease in silicate-Fe(III) and a concurrent increase in silicate-Fe(II) yielding a Fe(II)/Fe(III) ratio that was significantly higher than the pristine sediment (~0.6 vs. 0.3). The amount of biogenic silicate Fe(II) produced during the bioreduction experiment and measured by Mössbauer spectroscopy (8%, Table 1) corresponded to the 0.5 N HCl extractable Fe(II) produced during bioreduction (73.7 μmol/g, or ~9% of the total Fe concentration). Therefore, for this sediment, biogenic silicate Fe(II) can be extracted by 0.5 N HCl extraction even though little silicate Fe(II) in the pristine (unreduced) sediment was extracted in 0.5 N HCl (Table 1). The extent of silicate-Fe(III) reduction was similar to that noted in the FRC sediment after incubation with *S. putrefaciens* (strain CN32), despite different media composition and electron donor (Kukkadapu et al., 2006). In addition, the silicate Fe(II)/Fe(III) ratio was similar to that when the sediment was bioreduced with AQDS in the medium (rate and extent of goethite reduction, on the other hand, was enhanced in the presence of AQDS) and chemically reduced with dithionite-citrate-bicarbonate (DCB) (Kukkadapu et al., 2006) indicating that maximum silicate-Fe(III) reduction was obtained. The absence of soluble Si as a reduction byproduct was consistent with this hypothesis. The

Table 1 – Fe and Mn 0.5 N HCl extraction data and Mössbauer summary from the original (pristine) sediment, reduced sediment and re-oxidized sediment. HCl extractions times were 21–22 h (Fe) and 24 h (Mn)

Sediment	0.5 N HCl extraction data (μmol/g dry sediment)				Mössbauer summary			
	Fe(II)	Total Fe	Mn(II)	Total Mn	Silicate Fe(II) (%)	Silicate Fe(III) (%)	Goethite (%)	Hematite (%)
Pristine	0.4±0.1 (3)	30.4±0.8 (4)	2.9±0.2 (3)	33.4±7.8 (3)	10	35	53	2
Reduced	74.1±15.2 (6)	75.6±18.1 (6)	—	—	18	28	53	1
Re-oxidized	40.3±12.8 (12)	56.2±7.1 (13)	22.1±2.7 (6)	21.5±1.7 (6)	13	33	51	3

Data is average ± std. () denotes number of replicate samples.

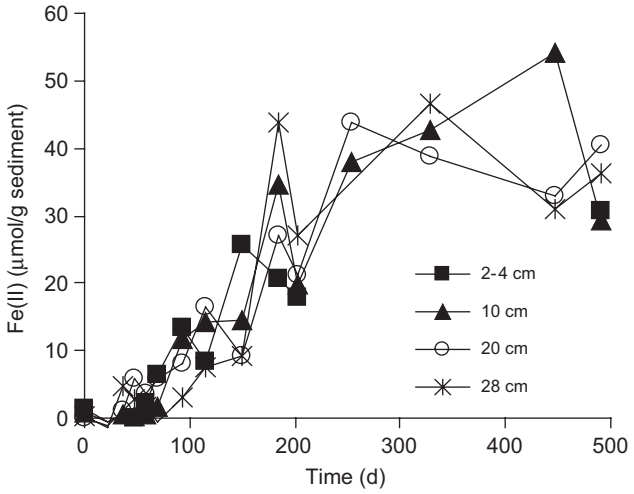

Fig. 2 – Surface bound Fe(II) concentrations (1 h extraction) over time during bioreduction for different locations along the 30 cm column (adapted from Komlos and Jaffé, 2004).

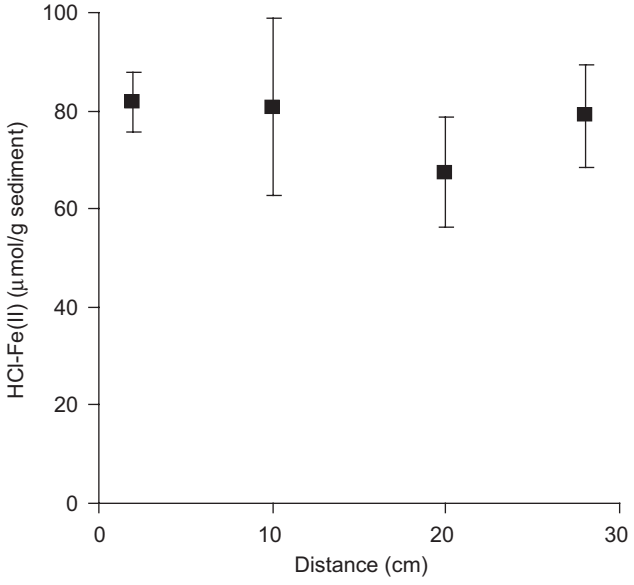

Fig. 3 – HCl-Fe(II) (22 h extraction) concentrations along the length of the column after 497 days of bioreduction (average ± std, $n = 3$).

results obtained here differ from those presented by Dong et al. (2003), where AQDS was required to reduce silicate Fe(III) (illite). Fe content and layer charge have been shown to play a significant role in illite reduction (Seabaugh et al., 2006) and could explain this discrepancy. The absence of discernable change to the relative spectral area of goethite after bioreduction (Figs. 1a and b) implied that goethite was not significantly reduced. The lack of goethite reduction corresponds to batch experiments using FRC sediment (Kukkadapu et al., 2006) but contradicts other biostimulation research using FRC sediment (Stucki et al., 2007). The reasons for the discrepancies are not clear but appear not to be due to variation in sediment mineralogy (Stucki et al., 2007) and may be due to changes in electron donor supplied, microbial communities (North et al., 2004), redox conditions, water chemistry, or subtle changes in mineralogy (crystallinity and Al-content of oxides, and Fe content and layer charge of illites, etc.). The reduced sediment analyzed in Fig. 1b was from the influent end of the column. Another sample analyzed by Mössbauer spectroscopy from the effluent end of the column revealed no significant difference in Fe valence ratios or phase distribution (data not shown) agreeing with the conclusion of a uniform Fe(II) concentration throughout the column after bioreduction as measured by chemical analysis (Fig. 3). The uniform spatial profile resulting from Fe(III)-silicate reduction was different than the banding of multiple Fe phases (magnetite, green-rust, vivianite) observed during ferrihydrite reduction under advective flow (Hansel et al., 2003).

There was no significant difference between the HCl-Fe(II) and HCl-Fe concentration after 22 h extraction (74.1±15.2 and 75.6±18.1 μmol/g dry sediment, respectively [$n = 6$]), indicating that no measurable Fe(III) was extracted. The lack of 0.5 N extractable Fe(III) present in the reduced sediment indicated that only those Fe-silicate domains that were fully reduced were soluble in 0.5 N HCl (also observed in Kukkadapu et al., 2006). Weak acid (0.5 N HCl) extraction for at least 1 h has been shown to solubilize siderite, vivianite, and green rust (Fredrickson et al., 1998; Kukkadapu et al., 2005), possible biogenic products of Fe(III)-oxide transformation (Zachara et al., 2002). The absence of Fe(III) in the HCl/hydroxylamine extractions of the reduced sediment indicated that the

biogenic Fe(II) was not in the form of green rust or magnetite, Fe(II)/Fe(III) phases. In addition, Mössbauer analyses did not show the presence of vivianite [$Fe_3(PO_4)_2$] or siderite [$FeCO_3$] which display significantly different Mössbauer spectra than silicate-Fe(II) and goethite (Wade et al., 1999; Jorand et al., 2000). Vivianite was an expected biogenic phase because a phosphate buffered medium was used to stabilize pH for the duration of the bioreduction. Vivianite forms as a product of the bacterial reduction of ferrihydrite, goethite and hematite when phosphate is present (Zachara et al., 1998; Fredrickson et al., 1998; Kukkadapu et al., 2004).

3.3. *Sediment re-oxidation with aerated PB solution*

3.3.1. *Dissolved oxygen profiles*

The reduced sediment was re-oxidized by continuously pumping aerated PB solution (without acetate) through the column. The measured DO of the influent solution was 7.1 ± 0.1 mg/L. A bromide breakthrough curve that was performed during the column experiment measured the pore volume (PV) and average hydraulic retention time of the column to be 11 mL and 30 min, respectively. The breakthrough of the majority of the bromide ($C/C_0 = 0.89$) occurred within two PV with complete breakthrough ($C/C_0 > 0.99$) occurring within 6 PV (Fig. 4).

Initially, effluent DO concentrations were significantly lower than influent DO concentrations (effluent DO was less than 0.2 mg/L for the first 26 PV). A sharp increase in effluent DO was measured between 26 and 75 PV (Fig. 4), after which the majority of the DO (6.2 mg/L, or 92% of the influent DO) exited the column. The effluent DO reached a pseudo steady-state concentration of 6.7 ± 0.1 mg/L ($n = 15$) (equivalent to 92.9 ± 1.8% of the influent DO) after 1700 PV. Therefore, re-oxidation of the bioreduced sediment displayed an initial fast oxidation step followed by a much slower one (long DO trailing, which was not observed in the bromide breakthrough curve) (Fig. 4). Though the bromide breakthrough curve did indicate the presence of a diffusion-limiting process given its non-symmetry (Fig. 4, insert), the bromide outflow concentration reached the value of the inflow concentration within seven PV, which was not achieved for DO over the entire duration of the experiment. This indicates that the shape of the DO breakthrough curve is a combined effect of diffusion and reaction limitations.

3.3.2. *HCl-Fe analysis*

The column was destructively sampled after 3900 pore volumes (81 days) of aerated PB solution were pumped through it when it appeared that pseudo steady-state conditions persisted and the effluent DO concentrations remained constant. The HCl-Fe(II) and HCl-Fe data (Fig. 5) indicate that more Fe(II) oxidation occurred in the middle and end of the column than in the beginning of the column. These non-uniform Fe(II) concentrations were due to the diffusion and reaction limitations described above. Using the average HCl-Fe(II) concentrations from the reduced and re-oxidized

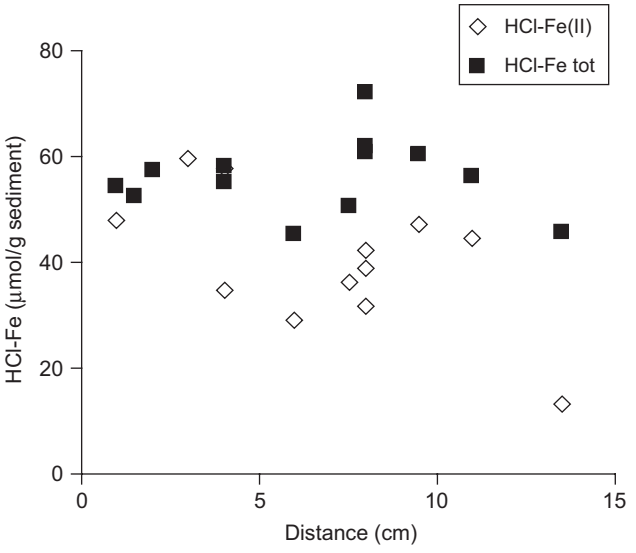

Fig. 5 – HCl-Fe(II) and HCl-Fe (21 h extraction) concentrations along the length of the column after re-oxidation.

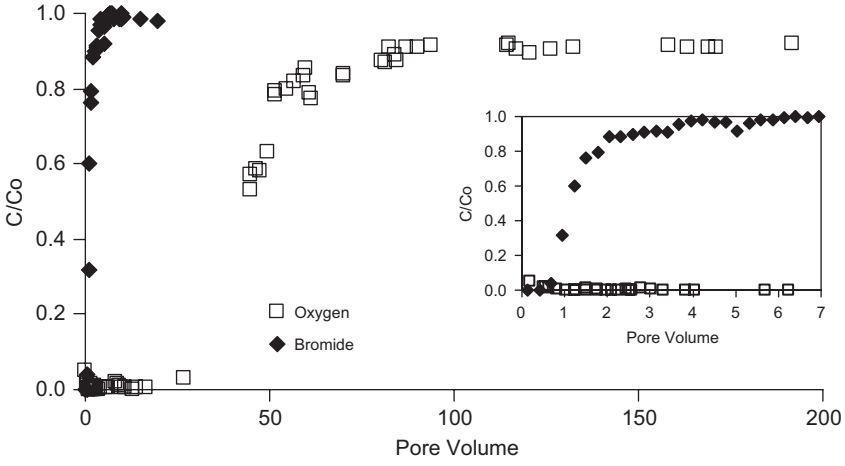

Fig. 4 – Effluent dissolved oxygen concentrations and bromide (tracer) concentrations versus pore volume of aerated buffered solution passed through column.

sediment (Table 1), the total amount of Fe(II) oxidized during the re-oxidation column experiment was calculated to be 33.8 μmol Fe(II)/g dry sediment [or 46% of the biogenic Fe(II)].

The remaining sediment from the re-oxidation column experiment was stored at 4 °C in a flask open to the atmosphere for 21 d followed by purging with air for three hours in an attempt to oxidize any remaining biogenic Fe(II) in the sediment. The HCl-Fe(II) present after this additional oxidation step was 18.3 (±0.5, $n = 5$) μmol Fe(II)/g dry sediment. Periodic sampling of the re-oxidized sediment over the next 14 d indicated that the Fe(II) concentration remained constant.

Comparison of the HCl-extractable Fe(II) before and after oxidation indicate that 46% of the biogenic Fe(II) was re-oxidized in the column, 30% of the biogenic Fe(II) was not oxidized in the column but was oxidized under completely mixed conditions, and 24% was kinetically unreactive with molecular oxygen, or reacted at an extremely slow rate.

3.3.3. *Mössbauer spectroscopy*

The Mössbauer spectrum for the re-oxidized sediment (Fig. 1c) was collected from a sample that underwent the additional aeration step after being removed from the column. This sample was chosen to represent fully re-oxidized, bioreduced sediment. Re-oxidation of the sediment increased the central Mössbauer doublet attributable to silicate-Fe(III) (Figs. 1b and c). This coincided with a loss of Fe(II) as measured by both a decrease in the silicate/bioreduced Fe(II) fraction of the Mössbauer spectrum (Fig. 1b and c) and a decrease in the Fe(II) measured using HCl extraction (Table 1). The HCl-Fe(II) and HCl-Fe concentration throughout the column after oxidation (40.3 ± 12.8 and 56.2 ± 7.1 μmol/g sediment, respectively) was lower (p-value < 0.02) than the HCl-Fe(II) concentration at the beginning of the re-oxidation experiment (74.1 ± 15.2 μmol/g sediment), indicating that the biogenic Fe(II) was partially oxidized to a form of Fe(III) not readily extractable in 0.5 N HCl. The absence of Fe(III) in acid-extracts and the lack of Mössbauer features at 12 K that are characteristic of ferrihydrite (Murad et al., 1988) suggested that ferrihydrite, a phase expected to form upon oxidation of adsorbed Fe(II), green rust, etc.; was not produced. All combined, the results indicate that, even though the sediment contained Fe(III)-oxides and Fe(III)-silicates, the majority of the Fe(III) that was bioreduced was structural silicate-Fe(III). The silicate-Fe(III) was reduced to silicate-Fe(II) during bioreduction and the biogenic silicate-Fe(II) was oxidized back to silicate-Fe(III) upon exposure to oxygen.

3.4. *Fe reduction in pristine and re-oxidized sediments*

Batch experiments with AQDS were performed to compare Fe reduction in the pristine sediment with the re-oxidized sediment (e.g., Fig. 1c). An increase in weak-acid extractable Fe(II) was measured within 5 days of incubation in the batch cultures containing re-oxidized sediment (Fig. 6). After 12 days of incubation, significantly more biogenic Fe(II) was produced in the re-oxidized sediment compared to the pristine one. Therefore, over the duration of this experiment, the re-oxidized Fe(III) was reduced more readily than the oxidized Fe(III) present in the pristine sediment. Two explanations for these results are: (i) the Fe(III) phase formed during oxidation of the reduced sediment was more bioavailable then the original form and/or (ii) a more energetically favorable electron acceptor (i.e. reducible Mn(III/IV) oxides) was present at higher levels in the pristine sediment and functioned as a temporary redox buffer. The Mössbauer and chemical analysis show no discernable mineralogic differences between regenerated Fe(III) in the re-oxidized sediment and mineral Fe(III) in the pristine sediment. Hence the bioavailability of the Fe(III) phases should have been comparable in the pristine and re-oxidized sediment.

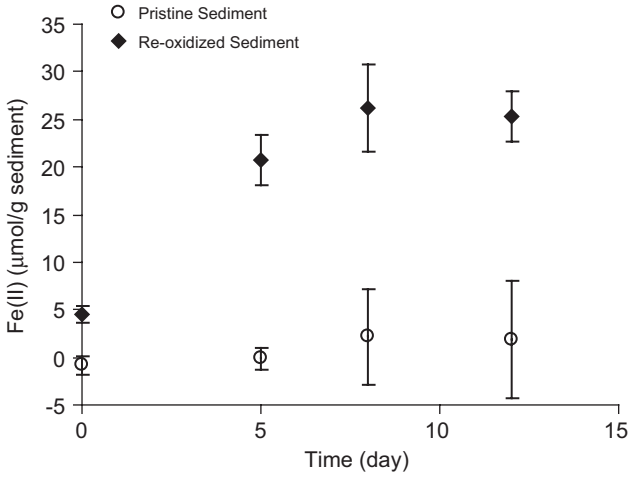

Fig. 6 – Batch iron reduction experiments with AQDS using the original (pristine) sediment (o) and the re-oxidized sediment (♦). Fe(II) values are an average of samples taken from three separate test tubes (±SD) and extracted for 1 h in 0.5N HCl.

To explore the influence of Mn on Fe reduction, pristine and re-oxidized sediment samples were analyzed for the presence of Mn(II) and total Mn. There was less total Mn (p-value < 0.05) in the re-oxidized sediment than the pristine sediment (Table 1), indicating that some soluble Mn was flushed out of the column. In addition, the Mn(II) present in the pristine sediment was only a small percentage (8.7%) of the total Mn concentration, while virtually all of the extractable Mn in the re-oxidized sediment was in the form of Mn(II) (Table 1). Therefore, the pristine sediment contained significant amounts of oxidized Mn that was reduced to Mn(II) during the bioreduction column experiment. Unlike Fe(II), however, the Mn(II) present in the bioreduced sediment did not re-oxidize when exposed to oxygenated water. The oxidation of Mn(II) by molecular oxygen is well-known to be kinetically limited (Davies and Morgan, 1989) and under certain conditions Mn(II) can be stable in the presence of dissolved oxygen for periods in excess of 7 years (Diem and Stumm, 1984). In addition, oxidized Mn has been shown to inhibit net Fe(II) production (Lovley and Phillips, 1988b; Myers and Nealson, 1988). Therefore, the apparent delay of Fe(II) production in the pristine sediment relative to the re-oxidized, bioreduced sediment appears to result from the presence of oxidized Mn (which was not detected in the re-oxidized sediment).

A longer duration batch experiment was performed without AQDS to determine how the rate of Fe(II) production would compare in the two sediments. Though the onset of Fe(II) production in the re-oxidized sediment (16.7 ± 4.0 d, $n = 3$) occurred before the pristine sediment (29.5 ± 9.2 d, $n = 2$), the rate of Fe reduction was comparable between the two sediments (0.54 ± 0.09 μmol/g/d and 0.57 ± 0.03 μmol/g/d for the pristine and re-oxidized sediment, respectively). Comparable Fe reduction rates were expected given that the Mössbauer analysis indicated that the Fe(III) in the two sediments were not mineralogically discernable from each other.

4. Conclusions

1. This study has shown that even though there were multiple Fe(III) phases [goethite, Fe(III)-silicates, hematite] present in this sediment, Fe(III)-silicates were preferentially reduced.
2. The Fe phases after bioreduction were uniform throughout the column indicating that Fe(II) was not significantly transported.
3. The extent of silicate-Fe(III) reduction in the column experiment was similar to that observed in batch experiments (which are easier to perform) as well as chemical (DCB) reduction indicating that the less time-consuming DCB extraction would be a good indicator of silicate-Fe(III) reduction potential in this sediment.
4. The biogenic silicate-Fe(II) was re-oxidized to silicate-Fe(III) that was mineralogically similar to the original (pristine) sediment.
5. Bioreduction of the cycled Fe(III) resulted in faster Fe(II) accumulation than in the pristine sediment. This was attributed to the absence of oxidized Mn (which was reduced during the initial bioreduction and was not re-oxidized when exposed to dissolved oxygen).
6. For these sediments in which the silicate-Fe(III) is the dominant form of reducible Fe(III), biogenic Fe(II) will be surface bound and not significantly exported from the system. This, coupled with the results that biogenic Fe(II) will re-oxidize back to silicate Fe(III), indicates that Fe can be cycled many times before the reducible Fe(III) in the system is exhausted.

Acknowledgments

This research was funded by the Natural and Accelerated Bioremediation Research (NABIR) program, Office of Biological and Environmental Research (OBER), US Department of Energy (DOE; Grants no. DE-FG02-00ER1263031 and DE-FG02-05ER63973). Mössbauer analysis was performed within the W. R. Wiley Environmental Molecular Sciences Laboratory (EMSL), a national user facility sponsored by the US DOE-OBER and located at Pacific Northwest National Laboratory (PNNL). PNNL is operated for the DOE by Battelle. The *Geobacter sulfurreducens* strain used was provided by Derek Lovley (U. of Mass., Amherst).

REFERENCES

Anderson, R.T., Rooney-Varga, J.N., Gaw, C.V., Lovley, D.R., 1998. Anaerobic benzene oxidation in the Fe(III) reduction zone of petroleum contaminated aquifers. Environ. Sci. Technol. 32, 1222–1229.

Anderson, R.T., Vrionis, H.A., Ortiz-Bernad, I., Resch, C.T., Long, P.E., Dayvault, R., Karp, K., Marutzky, S., Metzler, D.R., Peacock, A., White, D.C., Lowe, M., Lovley, D.R., 2003. Stimulating the in situ activity of *Geobacter* species to remove uranium from the groundwater of a uranium-contaminated aquifer. Appl. Environ. Microbiol. 69, 5884–5891.

Canfield, D.E., Thamdrup, B., Hansen, J.W., 1993. The anaerobic degradation of organic-matter in Danish coastal sediments—iron reduction, manganese reduction, and sulfate reduction. Geochim. Cosmochim. Acta 57 (16), 3867–3883.

Cooper, D.C., Neal, A.L., Kukkadapu, R.K., Brewe, D., Coby, A., Picardal, F.W., 2005. Effects of sediment iron mineral composition on microbially mediated changes in divalent metal speciation: Importance of ferrihydrite. Geochim. Cosmochim. Acta 69 (7), 1739–1754.

Davies, S.H.R., Morgan, J.J., 1989. Manganese(II) oxidation kinetics on metal oxide surfaces. J. Colloid Interf. Sci. 129, 63–77.

Diem, D., Stumm, W., 1984. Is dissolved Mn^{2+} being oxidized by O_2 in absence of Mn-bacteria or surface catalysts? Geochim. Cosmochim. Acta 48, 1571–1573.

Dong, H.G., Kukkadapu, R.K., Frederickson, J.K., Zachara, J.M., Kennedy, D.W., Kostandarithes, H.M., 2003. Microbial reduction of structural Fe(III) in illite and goethite. Environ. Sci. Technol. 37, 1268–1276.

Favre, F., Stucki, J.W., Boivin, P., 2006. Redox properties of structural Fe in ferruginous smectite. A discussion of the standard potential and its environmental implications. Clays Clay Miner 54 (4), 466–472.

Fredrickson, J.K., Zachara, J.M., Kennedy, D.W., Dong, H.L., Onstott, T.C., Hinman, N.W., Li, S.M., 1998. Biogenic iron mineralization accompanying the dissimilatory reduction of hydrous ferric oxide by a groundwater bacterium. Geochim. Cosmochim. Acta 62, 3239–3257.

Fredrickson, J.K., Zachara, J.M., Kennedy, D.W., Kukkadapu, R.K., McKinley, J.P., Heald, S.M., Liu, C., Plymale, A.E., 2004. Reduction of TcO4—by sediment-associated biogenic Fe(II). Geochim. Cosmochim. Acta 68, 3171–3187.

Gates, W.P., Stucki, J.W., Kirkpatrick, R.J., 1996. Structural properties of reduced Upton montmorillonite. Phys. Chem. Miner. 23, 535–541.

Hansel, C.M., Benner, S.G., Neiss, J., Dohnalkova, A., Kukkadapu, R.K., Fendorf, S., 2003. Secondary mineralization pathways induced by dissimilatory iron reduction of ferrihydrite under advective flow. Geochim. Cosmochim. Acta 67, 2977–2992.

Istok, J.D., Senko, J.M., Krumholz, L.R., Watson, D., Bogle, M.A., Peacock, A., Chang, Y.J., White, D.C., 2004. In situ bioreduction of technetium and uranium in a nitrate-contaminated aquifer. Environ. Sci. Technol. 38, 468–475.

Jaisi, D.P., Kukkadapu, R.K., Eberl, D.D., Dong, H., 2005. Control of Fe(III) site occupancy on the rate and extent of microbial reduction of Fe(III) in nontronite. Geochim. Cosmochim. Acta 69, 5429–5440.

Jorand, F., Appenzeller, B.M.R., Abdelmoula, M., Refait, P., Block, J.C., Génin, J.M.R., 2000. Assessment of vivianite formation in Shewanella putrefaciens culture. Environ. Technol. Lett. 21, 1001–1005.

Komlos, J., Jaffé, P.R., 2004. Effect of iron bioavailability on dissolved hydrogen concentrations during microbial iron reduction. Biodegradation 15, 315–325.

Kukkadapu, R.K., Zachara, J.M., Smith, S.C., Fredrickson, J.K., Liu, C.X., 2001. Dissimilatory bacterial reduction of Al-substituted

goethite in subsurface sediments. Geochim. Cosmochim. Acta 65, 2913–2924.

Kukkadapu, R.K., Zachara, J.M., Fredrickson, J.K., Kennedy, D.W., 2004. Biotransformation of two-line silica-ferrihydrite by a dissimilatory Fe(III)-reducing bacterium: formation of carbonate green rust in the presence of phosphate. Geochim. Cosmochim. Acta 68, 2799–2814.

Kukkadapu, R.K., Zachara, J.M., Fredrickson, J.K., Kennedy, D.W., Dohnalkova, A.C., McCready, D., 2005. Ferrous hydroxy carbonate is a stable transformation product of biogenic magnetite. Am. Mineral. 90, 510–515.

Kukkadapu, R.K., Zachara, J.M., Fredrickson, J.K., McKinley, J.P., Kennedy, D.W., Smith, S.C., Dong, H., 2006. Reductive biotransformation of Fe in shale-limestone saprolite containing Fe(III) oxides and Fe(II)/Fe(III) phyllosilicates. Geochim. Cosmochim. Acta 70, 3662–3676.

Larsen, O., Koch, B., 2000. Application of ^{57}Fe-enriched synthetic ferrihydrite to speciate the product of bacterial reduction. Hyperfine Interact. 126, 225–234.

Lovley, D.R., Phillips, E.J.P., 1987. Rapid assay for microbially reducible ferric iron in aquatic sediments. Appl. Environ. Microbiol. 53, 1536–1540.

Lovley, D.R., Phillips, E.J.P., 1988a. Novel mode of microbial energy metabolism: organic carbon oxidation coupled to dissimilatory reduction of iron or manganese. Appl. Environ. Microbiol. 54, 1472–1480.

Lovley, D.R., Phillips, E.J.P., 1988b. Manganese inhibition of microbial iron reduction in anaerobic sediments. Geomicrobiol. J. 6, 145–155.

Murad, E., Cashion, J., 2004. Mössbauer Spectroscopy of Environmental Materials and their Industrial Utilization. Kluwer Academic Publishers, Dordrecht.

Murad, E., Bowen, L.H., Long, G.J., Quin, T.G., 1988. The influence of crystallinity on magnetic-ordering in natural ferrihydrites. Clay Miner. 23, 161–173.

Myers, C.R., Nealson, K.H., 1988. Microbial reduction of manganese oxides: Interactions with iron and sulfur. Geochim. Cosmochim. Acta 52, 2727–2732.

North, N.N., Dollhopf, S.L., Petrie, L., Istok, J.D., Balkwill, D.L., Kostka, J.E., 2004. Change in bacterial community structure during in situ biostimulation of subsurface sediment contaminated with uranium and nitrate. Appl. Environ. Microbiol. 70, 4911–4920.

Peacock, A.D., Chang, Y.J., Istok, J.D., Krumholz, L., Geyer, R., Kinsall, B., Watson, D., Sublette, K.L., White, D.C., 2004. Utilization of microbial biofilms as monitors of bioremediation. Microb. Ecol. 47, 284–292.

Peretyazhko, T., Sposito, G., 2005. Iron(III) reduction and phosphorous solubilization in humid tropical forest soils. Geochim. Cosmochim. Acta 69, 3643–3652.

Rancourt, D.G., Ping, J.Y., 1991. Voigt-based methods for arbitrary-shape static hyperfine parameter distributions in Mössbauer spectroscopy. Nucl. Instr. Methods Phys. Res. B. 58, 85–97.

Roden, E.E., Zachara, J.M., 1996. Microbial reduction of crystalline iron(III) oxides: influence of oxide surface area and potential for cell growth. Environ. Sci. Technol. 30, 1618–1628.

Seabaugh, J.L., Dong, H., Kukkadapu, R.K., Eberl, D.D., Morton, J.P., Kim, J., 2006. Microbial reduction of Fe(III) in the Fithian and Muloorina illites: contrasting extents and rates of bioreduction. Clays Clay Miner. 54, 69–81.

Stucki, J.W., Lee, K., Goodman, B.A., Kostka, J.E., 2007. Effects of in situ biostimulation on iron mineral speciation in a sub-surface soil. Geochim. Cosmochim. Acta 71, 835–843.

Tuccillo, M.E., Cozzarelli, I.M., Herman, J.S., 1999. Iron reduction in the sediments of a hydrocarbon-contaminated aquifer. Appl. Geochem. 14, 655–667.

Van Cappellen, P., Wang, Y., 1996. Cycling of iron and manganese in surface sediments: a general theory for the coupled transport and reaction of carbon, oxygen, nitrogen, sulfur, iron, and manganese. Am. J. Sci. 296, 197–243.

Wade, M.L., Agresti, D.G., Wdowiak, T.J., Armendarez, L.A., 1999. Mössbauer investigation of iron-rich terrestrial hydrothermal vent systems: lessons for Mars exploration. J. Geophys. Res. 104, 8489–8507.

Zachara, J.M., Fredrickson, J.K., Li, S.M., Kennedy, D.W., Smith, S.C., Gassman, P.L., 1998. Bacterial reduction of crystalline Fe^{3+} oxides in single phase suspensions and subsurface materials. Am. Mineral. 83, 1426–1443.

Zachara, J.M., Kukkadapu, R.K., Fredrickson, J.K., Gorby, Y.A., Smith, S.C., 2002. Biomineralization of poorly crystalline Fe(III) oxides by dissimilatory metal reducing bacteria (DMRB). Geomicrobiol. J. 19, 179–207.

Zachara, J.M., Kukkadapu, R.K., Gassman, P.L., Dohnalkova, A., Fredrickson, J.K., Anderson, T., 2004. Biogeochemical transformation of Fe minerals in a petroleum-contaminated aquifer. Geochim. Cosmochim. Acta 68 (8), 1791–1805.